# Synthesis, Structure, and Bonding of $A_5Cd_2Tl_{11}$, A = Cs, Rb. Naked Pentagonal Antiprismatic Columns Centered by Cadmium

**Stefan Kaskel and John D. Corbett***

Ames Laboratory—DOE[1] and Department of Chemistry, Iowa State University, Ames, Iowa 50011

*Received January 18, 2000*

A new anionic thallium cluster chain $^1_\infty[Cd_2Tl_{11}^{5-}]$ has been discovered in the A−Cd−Tl systems for A = Cs, Rb. The compounds are synthesized by direct fusion of the elements at 700 °C and equilibration of the quenched product at 200 °C for 1 month. The thallides crystallize in the orthorhombic space group *Amm*2, $Z = 2$, $a =$ 5.6107(7) and 5.5999(6) Å, $b =$ 18.090(3) and 17.603(3) Å, $c =$ 13.203(3) and 12.896(2) Å for A = Cs and Rb, respectively, and contain chains of face-sharing pentagonal $Tl_{10}$ antiprisms embedded in a matrix of alkali metal cations. Cadmium atoms occupy the center of the antiprisms and donate electrons to the anionic chain. Additional four-bonded Tl atoms on one side of the chain make the structure acentric. The compounds are diamagnetic ($\chi_{296} = -0.8, -4.0$ ($\times 10^{-4}$) emu/mol, respectively) and metallic (10−20 $\mu\Omega$ cm at 275 K), and the indirect band gap energy of both compounds is close to zero according to extended Hückel calculations on the isolated chain.

## Introduction

In recent years, considerable effort has been spent investigating the formation and properties of tubelike morphologies with nanometer dimensions because of their potential applications in nanodevices and composite materials.[2] In this context, however, little attention has so far been paid to the fact that one-dimensional polyatomic chains are also immanent features of a huge variety of inorganic crystal structures, both in largely ionic compounds and in intermetallic compounds. Although these low-dimensional features are usually lost during dissolution of saltlike compounds, some metal cluster compounds may maintain certain configurations even in the melts.[3] It therefore seems highly desirable to explore reaction conditions, counterion effects, and bonding in order to work toward rational designs of predetermined cluster geometries and dimensionalities.

A chemical reaction between a very electropositive metal and one of the group 13 or triel (Tr) metals (as well as those of groups 14 and 15) is most generally understood as a reduction of the triel element that gives rise to a partial depolymerization of the condensed close-packed metal structure into clusters, networks, etc. The amount and size of the reducing agent as well as the bonding in the resulting cluster regulate the degree of depolymerization and the cluster morphology. Therefore, low concentrations of alkali metals result in alkali-metal-intercalated triel networks, whereas the highest degree of reduction with the largest amount of alkali metal leads to small clusters $Tr_4^{8-}$, in $Na_2In$ for example.[4] Interestingly, up to now the greater degrees of reduction have usually been achieved with the lighter alkali metals,[5] which obviously originates with their higher charge-to-radius ratios, closer packing, and more covalent bonding that stabilize the more highly reduced units. The reducing powers of the alkali metals vary in the opposite direction, suggesting a reverse trend as observed in the present compounds. But cation influences on the important terms involving cation−anion interactions are more difficult to generalize and make any a priori prediction of phase stability relatively complicated.

Although a variety of isolated triel clusters as well as network structures have been discovered in recent years, only a few such compounds have been synthesized so far that contain cluster chains. In the following we report the first example of a naked anionic cluster chain, in this case in the Cs−Tl and Rb−Tl systems when the evidently essential interstitial element Cd is also present.

## Experimental Section

**Syntheses.** The general reaction techniques in welded tantalum tubes have been described elsewhere.[6] All operations were performed in $N_2$- or He- filled gloveboxes. Pure samples of $Cs_5Cd_2Tl_{11}$ and $Rb_5Cd_2Tl_{11}$ according to their powder patterns are prepared by the fusion of stoichiometric amounts of the elements (for T1 bar, 99.998% Johnson Matthey, cleaned under $N_2$; for Cs and Rb ampuled under argon, 99.8%; for Cd shot, 99.9999%, Alfa-Aesar) in tantalum tubes at 700 °C for 2 days followed by quenching to room temperature and further annealing at 200 °C for 1 month. By this procedure, brittle, silverish, and very air-sensitive materials are obtained. Needle-shaped single crystals (typically about 30 $\mu$m × 30 $\mu$m × 300 $\mu$m) are grown by slow cooling (2 °C/h) of the mixture from 700 to 550 °C with subsequent annealing at 550 °C (130 h) and slow cooling (5 °C/h) to room temperature. Precession photographs show that the long crystal edges are parallel to the $Cd_2Tl_{11}^{5-}$ columns and thus the short *a* axis of the structure. Attempts to prepare isotypic $Na_5Cd_2Tl_{11}$, $K_5Cd_2Tl_{11}$, $K_5Cd_2In_{11}$, $Rb_5Cd_2In_{11}$, $Cs_5Cd_2In_{11}$, $Rb_5Zn_2In_{11}$, and $Cs_5Zn_2In_{11}$ all failed.

(1) This research was supported in part by the Office of Basic Energy Sciences, Materials Sciences Division, U.S. Department of Energy. The Ames Laboratory is operated for DOE by Iowa State University under Contract W-7405-Eng-82.

(2) Terrones, M.; Hsu, W. K.; Kroto, H. W.; David, R. M. *Top. Curr. Chem.* **1999**, *199*, 189. Terrones, M.; Grobert, N.; Hsu, W. K.; Zhu, Y. Q.; Hu, W. B.; Terrones, H.; Hare, J. P.; Kroto, H. W.; Walton, D. R. M. *MRS Bull.* **1999**, *24*, 43. Nesper, R.; Muhr, H.-J. *Switz. Chim.* **1998**, *52*, 571. Tremel, W. *Angew. Chem., Int. Ed. Engl.* **1999**, *38*, 2l75.

(3) van der Lugt, W. In *Chemistry, Structure and Bonding of Zintl Phases and Ions*; Kauzlarich, S., Ed.; VCH Publishers: New York, 1996; p183. van der Aart, S. A. Nanometer Superstructure in Some Liquid Alloys. Ph.D. Thesis, Delft University Press: Delft, The Netherlands, 1998.

(4) Sevov, S. C.; Corbett, J. D. *J. Solid State Chem.* **1993**, *103*, 114.

(5) (a) Corbett, J. D. In *Chemistry, Structure and Bonding of Zintl Phases and Ions*; Kauzlarich, S., Ed.; VCH Publishers: New York, 1996; p 139. (b) Corbett, J. D. *Angew. Chem., Int. Ed. Engl.* **2000**, *39*, 670.

(6) Sevov, S. C.; Corbett, J. D. *Inorg. Chem.* **1991**, *30*, 4875.

10.1021/ic000061y CCC: $19.00 
Published on Web 06/17/2000

**Properties.** The magnetic susceptibilities of the compounds were measured between 6 and 296 K on a Quantum Design MPMS superconducting quantum interference device (SQUID) magnetometer at a field of 3 T. A quantity of 126.6 mg of $Cs_5Cd_2Tl_{11}$ (23.6 mg of $Rb_5Cd_2Tl_{11}$) was loaded in a He-filled glovebox into silica tubes where the samples were held between two silica rods. These were sealed under a partial vacuum. The susceptibility data were corrected for the sample holder and for the diamagnetic contributions of the atom cores ($-5.73 \times 10^{-4}$ emu/mol for Cs, $-5.18 \times 10^{-4}$ emu/mol for Rb). The corrected molar susceptibilities of the Cs salt are then $-1.33 \times 10^{-4}$ and $-0.84 \times 10^{-4}$ emu/mol at 11 and 296 K, respectively. The data show a small positive temperature dependence ($\partial\chi/\partial T = 1.70(3) \times 10^{-7}$ emu/(mol K)). The rubidium salt gave similar results, with $\chi_{11} = -4.5 \times 10^{-4}$ emu/mol, $\chi_{296} = -4.1 \times 10^{-4}$ emu/mol, and $\partial\chi/\partial T = 1.8(1) \times 10^{-7}$ emu/(mol K).

Resistivities of the phases were measured by the electrodeless Q method[7] on 54.5 (63.3) mg of the Cs (Rb) compound that had been sieved to a 250−425 $\mu$m powder and diluted with chromatographic $Al_2O_3$. Measurements were made at 34 MHz over 100−277 K. The resistivity of the Cs salt at 277 K is 11 $\mu\Omega$ cm, and the temperature coefficient is positive ($(\partial\rho/\partial T)/\rho = 1.1(1) \times 10^{-3}$ K$^{-1}$), while the rubidium compound yields 24 $\mu\Omega$ cm at 278 K with a temperature dependence of $1.8(1) \times 10^{-3}$ K$^{-1}$. Plots of both sets of these properties appear in the Supporting Information.

**Structure Determination.** Several crystals of $Cs_5Cd_2Tl_{11}$ were mounted in a $N_2$-filled glovebox into Mark capillaries, which were sealed, and the crystals were checked for singularity by means of Laue photos. Many regular-appearing blocks turned out to be in fact dense packings of smaller crystals. Finally, a needle-shaped crystal of approximate dimensions 30 $\mu$m × 30 $\mu$m × 240 $\mu$m was selected for the data collection. All measurements were made on a Rigaku AFC6R diffractometer with the aid of graphite monochromated Mo K$\alpha$ radiation from a rotating anode generator. Initial cell constants and the orientation matrix were obtained from a least-squares refinement using the setting angles of 21 reflections in the range $13° < 2\theta < 17°$. Diffraction data were collected at 23 °C using the $\omega$ scan technique to a maximum $2\theta$ value of 55°.

The TEXSAN[8] program package was used for data processing and structure solution. After Lorentz polarization and absorption corrections (three $\psi$ scans), intensity statistics, and systematic absences suggested an orthorhombic space group among *Cmcm*, *Cmc*$2_1$, or *Ama*2 (all with extinction symbols *C*-*c*- or equivalent). But in all cases, two large residual electron density peaks remained in the Fourier map following a solution and refinement, and these had an unreasonably short distance of 0.96 Å between them. A careful check of the extinction conditions showed that indeed two reflections in the data set for $Cs_5Cd_2Tl_{11}$ with $F^2/\sigma(F^2) = 4.5$ violated the *c*-glide condition, thus indicating that the true extinction symbol was *C*- - - (or *A*- - -, depending on the setting). These observations were also proven by means of precession photographs (*hk*0, *hkl*, *h*0*l*, *h*1*l*) especially for $Rb_5Cd_2Tl_{11}$ where the violation of -*c*- was clearly visible.

A successful solution was finally obtained in the acentric space group *Amm*2. The positions of the heaviest atoms (Tl1−Tl7) were obtained by means of direct methods using SHELXS.[9] The positions for Cd and Cs1−Cs3 were located from difference Fourier maps. After isotropic refinement of all positions, the *R* value was 6.05% and the highest electron density peak(s) was 6.5 e/Å$^3$, all within 1.1 Å of one of the heavier atoms. After the anisotropic refinement, analysis of the most disagreeable reflections showed that the worst deviations came from the four [011] reflections with observed intensities that were too small (for example, for $0\bar{1}1$, $F_o - F_c = -396.9(3.0)$). Since $2\theta = 3.82°$ for [011] was the smallest in the data set, it was concluded that these reflections had all suffered from interference by the beam stop, and they were thereafter excluded from the data set. After all reflections were averaged ($R_{av} = 9.3\%$), the refinement converged with $R = 3.5\%$, $R_w = 3.8\%$ with the highest residual electron density peak of 3.9 e/Å$^3$. All residual peaks had distances of less than 1.1 Å to one of the heavy atoms, so they were attributed to incomplete absorption corrections ($\mu$ = 740, 804 cm$^{-1}$). Friedel pairs were analyzed to determine the absolute structure of the compound. Out of 25 reflections, 19 with $[||F_c^+| - |F_c^-||/(\sigma^2(F_c^+) + \sigma^2(F_c^-))^{1/2}] > 1.0$ showed the correct trend (Flack parameter: 0.29(4)), indicating that the refined configuration was right and that a small amount of racemic twinning was present.

The lattice parameters used for the distance calculations were obtained by least-squares refinement of 20 reflections in the range $28 < 2\theta < 77°$ measured in the Guinier powder pattern (Cu K$\alpha_1$ radiation) with the aid of NIST silicon as an internal standard. These values were used for distance calculations.

Similar procedures were used in the structure solution of the Rb compound with one difference, that no reflection suffered from beam stop interference. Some crystallographic and refinement data are given in Table 1, while the positional and isotropic-equivalent displacement parameter data are listed in Table 2. Further refinement data and the anisotropic displacement parameters are contained in the Supporting Information. These as well as the $F_o/F_c$ listings are available from J.D.C.

**MO Calculations.** Band structure and MO calculations were performed at the extended Hückel level[10] using the CAESAR program

**Table 1.** Some Crystal and Refinement Data

| | | |
|---|---|---|
| empirical formula | $Cs_5Cd_2Tl_{11}$ | $Rb_5Cd_2Tl_{11}$ |
| fw | 3137.42 | 2900.23 |
| cryst syst, lattice type | orthorhombic, A-centered | |
| space group, *Z* | *Amm*2 (No. 38), 2 | |
| lattice parameters[a] | | |
| *a*, Å | 5.6107(7) | 5.5999(6) |
| *b*, Å | 18.090(3) | 17.603(3) |
| *c*, Å | 13.203(2) | 12.896(2) |
| *V*, Å$^3$ | 1340.0(3) | 1271.2(3) |
| $d_{calc}$, g/cm$^3$ | 7.775 | 7.576 |
| $\mu$(Mo K$\alpha$), cm$^{-1}$ | 739.9 | 804.3 |
| rel transm coeff range | 0.472−1.000 | 0.529−1.000 |
| $R_{int}$, $I > 3\sigma_I$ | 0.036 | 0.098 |
| residuals: *R*; $R_w$[b] | 0.035; 0.038 | 0.048, 0.044 |

[a] Refined from Guinier pattern with Si as internal standard. $\lambda$ = 1.540 562 Å, 23 °C. [b] $R = \sum||F_o| - |F_c||/\sum|F_o|$; $R_w = [\sum w(|F_o| - |F_c|)^2/\sum w(F_o)^2]^{1/2}$.

**Table 2.** Atomic Coordinates and $B_{eq}$ for $Cs_5Cd_2Tl_{11}$ and $Rb_5Cd_2Tl_{11}$[a]

| atom | wyckoff symbol, site symmetry | *x* | *y* | *z* | $B_{eq}$[b] |
|---|---|---|---|---|---|
| Tl1 | 2*a*, *mm2* | 0.0000 | 0.0000 | 0.2892 | 2.5(1) |
| | | | | 0.2893 | 2.3(1) |
| Tl2 | 4*d*, *m*.. | 0.0000 | 0.1559(2) | 0.1315(4) | 1.55(8) |
| | | | 0.1610(1) | 0.1309(4) | 2.05(7) |
| Tl3 | 4*e*, *m*.. | 0.5000 | 0.0988(2) | 0.2396(4) | 2.7(1) |
| | | | 0.1029(1) | 0.2437(4) | 2.19(7) |
| Tl4 | 4*d*, *m*.. | 0.0000 | 0.0972(2) | −0.1156(4) | 1.73(8) |
| | | | 0.0979(1) | −0.1203(4) | 2.16(6) |
| Tl5 | 2*b*, *mm*2 | 0.5000 | 0.0000 | −0.1583(3) | 1.6(1) |
| | | | | −0.1704(2) | 2.0(1) |
| Tl6 | 4*e*, *m*.. | 0.5000 | 0.1556(2) | −0.0056(5) | 2.7(1) |
| | | | 0.1595(1) | −0.0092(4) | 2.26(8) |
| Tl7 | 2*b*, *mm*2 | 0.5000 | 0.0000 | 0.4307(4) | 4.4(1) |
| | | | | 0.4384(4) | 4.67(9) |
| A1 | 4*d*, *m*.. | 0.0000 | 0.1895(3) | 0.4215(6) | 3.2(2) |
| | | | 0.1925(3) | 0.4142(6) | 3.1(2) |
| A2 | 2*a*, *mm*2 | 0.0000 | 0.0000 | 0.6261(7) | 5.2(2) |
| | | | | 0.6248(8) | 4.3(2) |
| A3 | 4*e*, *m*.. | 0.5000 | 0.3102(3) | 0.2033(6) | 3.8(2) |
| | | | 0.3120(3) | 0.1965(7) | 3.6(2) |
| Cd | 4*c*, .*m*. | 0.252(2) | 0.0000 | 0.0629(6) | 1.81(5) |
| | | 0.248(1) | | 0.0606(6) | 2.01(5) |

[a] The second parameter listed is for $Rb_5Cd_2Tl_{11}$. [b] $B_{eq} = (8/3)\pi^2[U_{11}(aa^*)^2 + U_{22}(bb^*)^2 + U_{33}(cc^*)^2]$.

(7) Zhao, J.-T.; Corbett, J. D. *Inorg. Chem.* **1995**, *34*, 378.
(8) *TEXSAN for Windows: Crystal Structure Analysis Package*; Molecular Structure Corporation: The Woodlands, TX, 1997.
(9) Sheldrick, G. M. *SHELX97*; University of Göttingen, Göttingen, Germany, 1997.
(10) Hoffmann, R. *J. Chem. Phys.* **1963**, *39*, 1397.

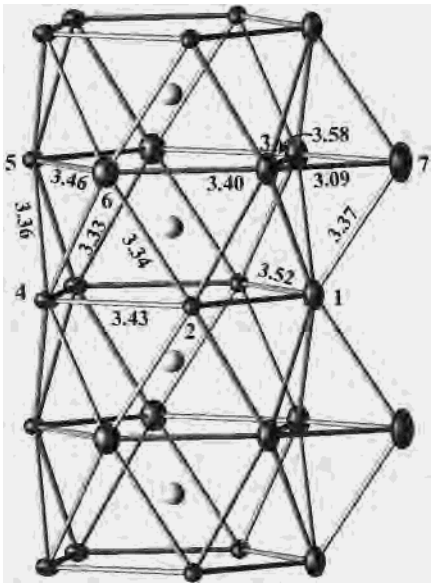


**Figure 1.** Portion of the one-dimensional infinite $Cd_2Tl_{11}$ column in $Cs_5Cd_2Tl_{11}$. Tl atoms 1, 5, 7 and Cd lie on a vertical mirror plane (50% probability ellipsoids). The lighter Cd atoms center the Tl antiprisms.

package developed by Whangbo et al.[11] Because the cations cannot be sensibly included, a single idealized icosahedral chain ($D_{5h}$ symmetry) was employed with Tl−Tl distances of 3.456 Å in the pentagonal bases, the average observed for the cesium salt. The stacking periodicity was 2.28 Å ($d$(Tl−Tl) = 3.356 Å). The Tl3−Tl7 distance between the idealized chain and the acentric Tl7 added later to examine its effect was set to 3.09 Å. The orbital energies used were derived from density functional theory.[12] Orbital energies $-H_{ii}$ (eV) and exponents $\xi$ for Cd[13] and Tl[14] were the following: Tl 6s 11.525, 2.37; Tl 6p 5.715, 1.97; Cd 5s 9.253, 1.64; Cd 5p 4.933, 1.60.

For calculations on the idealized chain, 400K points were used between Γ and X. For the final calculations on the observed, slightly distorted chain ($C_s$ symmetry), 1000K points were employed to ensure that avoided band crossings would not occur because the energies had been calculated at too few points.

## Results and Discussion

**Structure.** $Cs_5Cd_2Tl_{11}$ and $Rb_5Cd_2Tl_{11}$ represent a new and remarkable structure type. Pentagonal thallium antiprisms centered by cadmium atoms are stacked to share pentagonal faces and form columns along the short $a$ axis of the orthorhombic unit cell, as shown in Figure 1 for the cesium phase. The height of each antiprism is exactly $a/2$, and these units are virtually the same for both phases, the smaller size of rubidium being reflected almost entirely in the shorter $b$ and $c$ axes. All atoms but Cd lie on mirror planes normal to $a$ at $x = 0, {}^1/_2$, the shared faces of the antiprisms, while Tl1, Tl5, Tl7, A2, and Cd also lie on mirror planes at $y = 0, {}^1/_2$ that center the chains. In general, the anion portions in the two structures are very similar, ≤ 0.07 Å in the extreme (Table 3). This rigidity might be a reason good packing is not achieved for the hypothetical potassium compound. The columns are embedded in a matrix of cations and isolated from each other (Figure 2). The shortest distance between thallium atoms in two columns (Tl5−Tl7) is the comparatively long 5.43 Å for the Cs and 5.04 Å for the Rb compound, whereas the Tl−Tl separations within the anionic chains vary between 3.092 and 3.623 Å. The deviation of the columns from ideal 5-fold symmetry is small; the Tl−Tl distances within the planar pentagonal faces are almost uniform, 3.397−3.575 Å (Cs compound) and longer than the bonds between these faces (3.313−3.390 Å). Compared with an ideal icosahedron, the pentagonal antiprisms are therefore slightly compressed along the chain. The three largest bond length differences between the Cs and Rb salts, ≤ 0.07 Å, occur in the pentagonal faces and increase the former range slightly to 3.410−3.623 Å for Rb. The overall distances are comparable to those found in other naked icosahedral thallium clusters, e.g., in the centered isosahedron in $Na_3K_8Tl_{13}$, 3.273 Å to the center and 3.217−3.578 Å on the surface.[15] The Cd−Cd distances at 2.79 and 2.82 Å are comparable to those found in $K_{14}Cd_9Tl_{21}$ (2.816 Å),[16] while the 10 Cd−Tl distances are quite uniform and range from 3.24 to 3.30 Å.

**Table 3.** Distances (<4.59 Å) in $A_5Cd_2Tl_{11}$, A = Cs, Rb

| | | Cs | Rb |
|---|---|---|---|
| Tl1−Tl2 | 2× | 3.505(5) | 3.493(5) |
| Tl1−Tl3 | 4× | 3.390(3) | 3.386(2) |
| Tl1−Tl7 | 2× | 3.371(4) | 3.397(4) |
| Tl2−Tl1 | | 3.505(5) | 3.493(5) |
| Tl2−Tl3 | 2× | 3.313(3) | 3.317(3) |
| Tl2−Tl4 | | 3.430(6) | 3.425(6) |
| Tl2−Tl6 | 2× | 3.339(1) | 3.333(2) |
| Tl3−Tl1 | 2× | 3.390(3) | 3.386(2) |
| Tl3−Tl2 | 2× | 3.313(3) | 3.317(3) |
| Tl3−Tl3 | | 3.575(4) | 3.623(4) |
| Tl3−Tl6 | | 3.397(6) | 3.410(5) |
| Tl3−Tl7 | | 3.092(6) | 3.096(5) |
| Tl4−Tl2 | | 3.430(6) | 3.425(6) |
| Tl4−Tl4 | | 3.518(9) | 3.447(6) |
| Tl4−Tl5 | 2× | 3.359(3) | 3.351(2) |
| Tl4−Tl6 | 2× | 3.330(3) | 3.327(3) |
| Tl5−Tl4 | 4× | 3.359(3) | 3.351(2) |
| Tl5−Tl6 | 2× | 3.461(6) | 3.494(5) |
| Tl6−Tl2 | 2× | 3.339(1) | 3.333(2) |
| Tl6−Tl3 | | 3.397(6) | 3.410(5) |
| Tl6−Tl4 | 2× | 3.330(3) | 3.327(3) |
| Tl6−Tl5 | | 3.461(6) | 3.494(5) |
| Tl7−Tl1 | 2× | 3.371(4) | 3.397(4) |
| Tl7−Tl3 | 2× | 3.092(6) | 3.096(5) |
| Cd−Cd | | 2.82(2) | 2.82(2) |
| Cd−Cd | | 2.79(2) | 2.78(2) |
| Cd−Tl1 | | 3.30(1) | 3.26(1) |
| Cd−Tl2 | 2× | 3.280(7) | 3.285(6) |
| Cd−Tl3 | 2× | 3.253(9) | 3.293(8) |
| Cd−Tl4 | 2× | 3.262(9) | 3.216(8) |
| Cd−Tl5 | | 3.24(1) | 3.30(1) |
| Cd−Tl6 | 2× | 3.268(7) | 3.268(6) |
| A1−Tl1 | | 3.847(7) | 3.751(9) |
| A1−Tl2 | | 3.876(9) | 3.69(1) |
| A1−Tl2 | | 3.939(8) | 3.80(1) |
| A1−Tl3 | 2× | 4.040(6) | 3.894(7) |
| A1−Tl4 | | 3.889(9) | 3.717(8) |
| A1−Tl6 | 2× | 4.081(6) | 3.950(6) |
| A1−Tl7 | 2× | 4.431(5) | 4.407(5) |
| A2−Tl1 | | 4.45(1) | 4.33(1) |
| A2−Tl4 | 2× | 3.837(9) | 3.71(1) |
| A2−Tl5 | 2× | 3.996(8) | 3.85(1) |
| A2−Tl7 | 2× | 3.811(8) | 3.69(1) |
| A3−Tl2 | 2× | 4.070(6) | 3.953(6) |
| A3−Tl3 | | 3.854(9) | 3.731(9) |
| A3−Tl4 | 2× | 4.049(6) | 3.992(7) |
| A3−Tl5 | | 3.889(8) | 3.727(8) |
| A3−Tl6 | | 3.929(9) | 3.83(1) |
| A3−Tl6 | | 3.892(9) | 3.774(9) |
| A1−A2 | | 4.365(9) | 4.34(1) |
| A1−A3 | 2× | 4.575(4) | 4.489(7) |
| A2−A1 | 2× | 4.365(9) | 4.34(1) |
| A2−A3 | 4× | 4.549(6) | 4.432(8) |
| A3−A1 | 2× | 4.575(4) | 4.489(7) |
| A3−A2 | 2× | 4.549(6) | 4.432(8) |

(11) Ren, J.; Liang, W.; Whangbo, M.-H. *CAESAR*; PrimeColor Software, Inc.: Raleigh, NC, 1998.
(12) Vela, A.; Gazquez, J. L. *J. Phys. Chem.* **1988**, *92*, 5688.
(13) Alvarez, S. *Tables of Parameters for Extended Hückel Calculations*; Universität de Barcelona: Barcelona, Spain, 1989.
(14) Whangbo, M.-H. *Inorg. Chem.* **1990**, *29*, 257.
(15) Dong, Z.-C.; Corbett, J. D. *J. Am. Chem. Soc.* **1995**, *117*, 6447.

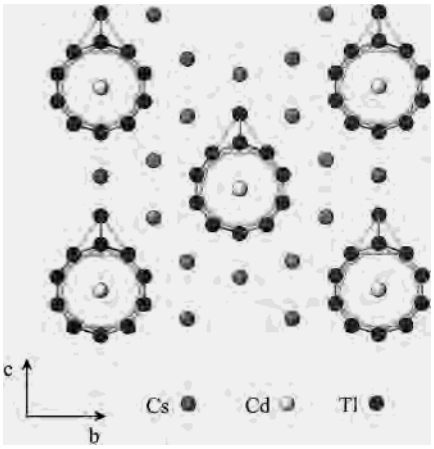


**Figure 2.** Projection of $Cs_5Cd_2Tl_{11}$ structure along the columns axis [100].

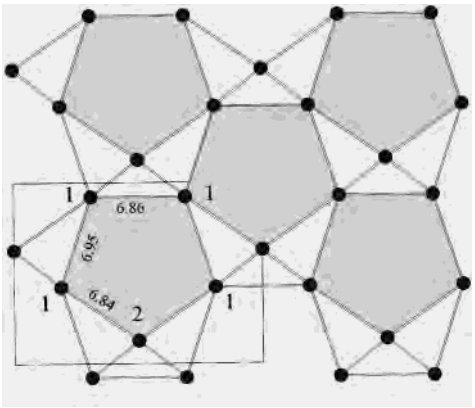


**Figure 3.** Cs ions form planar nets normal to [100] at $x = 0.0$ (shown) and 0.5 (not shown) of corner-sharing pentagons.

The distortions from 5-fold symmetry are caused by the additional Tl7 atoms present on one side of the naked anionic cluster chain that serve to cap and elongate one edge of the columns (Tl3−Tl3 = 3.575 (Cs), 3.623 (Rb) Å) and to make the structure acentric. The accompanying Tl7−Tl3 distances of 3.092 Å (3.096 Å) are the shortest Tl−Tl separations in the two phases. This is not especially surprising because Tl7 forms only four bonds to neighboring thallium atoms, whereas the other Tl atoms are six-, seven- or eight-bonded to like atoms. The other two bonds to the capping atom, Tl7−Tl1, are neither unusual for interpentagon values nor changed by the cation.

The icosahedral columns are separated from each other by a layer of cesium cations (Figure 2). All cations occupy edge-bridging positions on the pentagons with *x* parameters identical to those of the thallium atoms. They thus form nets at $x = 0$ (A1, A2) and at $x = 0.5$ (A3) that are coplanar with, or halfway between, the two pentagonal bases. The Cs−Tl distances in the same plane are only a little shorter (3.837−3.939 Å) than distances to atoms above and below (3.996−4.081 Å), while the Rb−Tl values are proportionately smaller.

In the planar net at $x = 0$, the Cs1 and Cs2 atoms define almost perfect corner-sharing pentagons (6.84−6.95 Å) surrounding the chains (Figure 3). Since pentagons alone cannot be packed periodically in two dimensions, the net also contains smaller irregular polygons, so the $A_5Cd_2Tl_{11}$ structure is an example how pentagonal columns can be arranged to form a crystalline pattern. The layer containing A3 at $x = 0.5$ is more distorted because of the intrusion of Tl7. The instability of this anion with potassium probably originates with the small cation, which can pack more efficiently around other polyanions.

(16) Tillard-Charbonnel, M.; Chahine, A.; Belin, C. *Z. Kristallogr.* **1995**, *210*, 162. Tillard-Charbonnel, M.; Chahine, A.; Belin, C.; Rousseau, R.; Canadell, E. *Chem.−Eur. J.* **1997**, *3*, 799.

**Table 4.** Character Table

| irreducible representation in $C_{5v}$ | s | p |
|---|---|---|
| $a_1$ | $a_s$ | $a_r\ a_z$ |
| $a_2$ | | $a_t$* |
| $e_1$ | $e_s$ | $e_r\ e_z\ e_t$* |
| $e_2$ | $e_s$* | $e_t\ e_z$* $e_r$* |

**Bonding.** A fundamental understanding of the structure−bonding relationships is most easily achieved at the simple extended Hückel MO level. Since the most important impact of cesium (rubidium) is the donation of its electrons to the $Cd_2Tl_{11}$ substructure, the $Cd_2Tl_{11}^{5-}$ chain was analyzed alone with a one-dimensional band calculation ($\mathbf{\Gamma} = 0,0,0$; $\mathbf{X} = {}^1/_2a^*,0,0$). An idealized pentagonal antiprismatic column ($D_{5h}$) was analyzed first, and then Cd and the Tl7 "fin" were added separately in order to understand the role of the central Cd as well as the addition of the unusual exoskeletal Tl7 that makes the structure acentric.

The description of such a pentagonal column in terms of an aggregation of cyclopentadienide anions has evidently not been provided before. To this end, the bands for ${}^1_\infty[Tl_{10}]$ columns are conveniently labeled according to their similarities to the MO's of the $Cp^-$ ring, which is isoelectronic with the (hypothetical) pentagonal $Tl_5^{11-}$. In $Tl_5^{11-}$, the 5s orbitals split in two bonding ($a_s$, $e_s$) and one antibonding ($e_s$*) levels. For the three p orbitals per Tl, it is convenient to have one radial ($p_r$) orbital oriented toward the center of the pentagon, one tangential ($p_t$) along a tangent of the outer circle, and the third ($p_z$) normal to the plane. The $p_z$ and $p_r$ orbitals split the same way as do the s orbitals ($a_z$, $e_z$, $e_z$*; $a_r$, $e_r$, $e_r$*), but the order of the $p_t$ orbitals is reversed ($e_t$, $e_t$*, $a_t$*). The result is basically five occupied lone-pair-like MO's ($a_s$, $e_s$, $e_s$*), three radial and two tangential bonding MO's ($a_r$, $e_r$, $e_t$) in plane, corresponding to five $\sigma$ bonds in the ring, and three $\pi$-type $p_z$ orbitals ($a_z$, $e_z$). This is the so-far-undiscovered $Tl_5^{11-}$ cluster if all 13 bonding MO's are occupied.

In the formal $(A^+)_5(Cd^{2+})_2(Tl_{11}^{9-})$, the total number of valence electrons per ring is ~20 (~$[Tl_5^{5-}]$), far lower than in the isolated $Tl_5^{11-}$, so a higher degree of aggregation is required. When $Tl_5$ rings stack to form antiprismatic stacked columns, as in our new naked cluster anion, each MO of $Tl_5$ gives rise to a folded band. (The $Tl_5^{11-}$ MO's and the dispersion of the five $p_z$ orbitals in the chain are illustrated in the Supporting Information.) The point group of the wave vector at the $\Gamma$ point is $D_{5h}$, whereas the point group of the wave vector is reduced (index 2) to $C_{5v}$ at an arbitrary *k* point $x\cdot\mathbf{a}^*$. Therefore, band mixing occurs in the one-dimensional Brillouin zone $\Gamma-X$ between bands derived from orbitals of the same irreducible representation in $C_{5v}$ (small representations). The character table (Table 4) shows that a-type MO's can be classified with respect to $\sigma_v$ whereas the degenerate e-type differ with respect to $C_5$. (*z* in the local MO picture becomes the $C_5$ axis of the chain.) In a general bonding picture, all s states are occupied. Among the p orbitals, the $a_r$ and the $a_z$ band mix to form a folded bonding and antibonding band whereas the $e_1$ ($e_r$, $e_z$, $e_t$*) and $e_2$ ($e_t$, $e_z$*, $e_r$*) bands mix to form one bonding and two antibonding folded bands, respectively (Figure 4). The number of bonding MO's is therefore reduced by three per five-membered ring, and an optimized bonding situation is achieved in an isolated ${}^1_\infty[Tl_{10}^{10-}]$ chain.

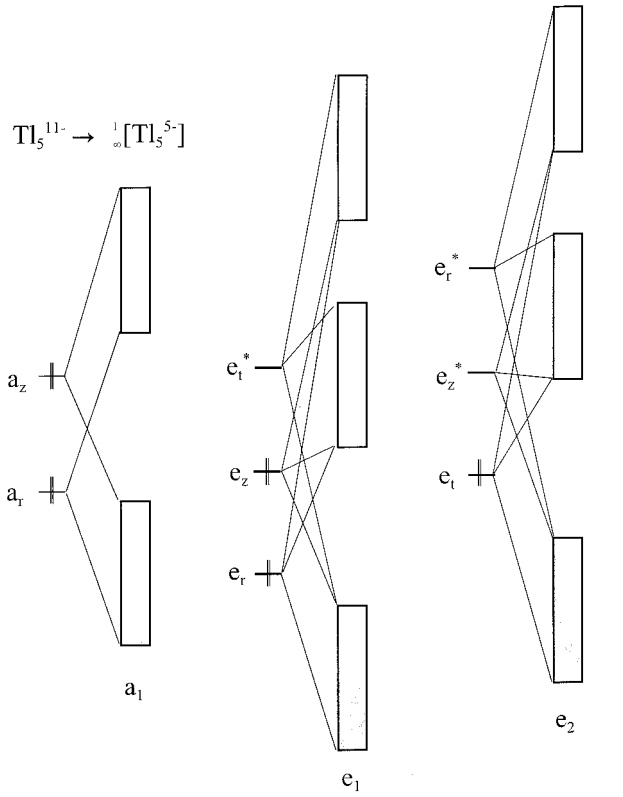


**Figure 4.** Overall mixing scheme for p orbitals in the $Tl_{10}$ chain. $\sigma$-bond formation along the stacking axis reduces the number of bonding p MO's (7) in $Tl_5^{11-}$ to five bonding bands per $Tl_5$ ring in the chain at the expense of radial and tangential bonds in the rings.

Interestingly, an optimized bonding situation would also be present in a pentagonal antiprismatic $Tl_{10}^{16-}$ cluster (an arachno Wade cluster) and in $Tl_{20}^{26-}$ composed of four such rings or two $Tl_{10}$ clusters. It is obvious that six electrons are lost (three MO's become antibonding) on dimerization of the two five rings or two arachno clusters, which is more easily understood as the combination of two five rings because the $a_z$ and $e_z$ orbitals combine to form one bonding and one antibonding level, respectively (simplified). Extending this construction to the infinite chain results in a ${}^1_\infty[Tl_{10}^{10-}]$ unit.

The staggered chain has 20 electrons per five-membered ring. A novel class of compounds with similar structural units is found in metal-rich chalcogenides of group 5 elements originally discovered by Franzen and Smeggil[17] and further explored recently in great detail by Harbrecht and co-workers as well as by Hughbanks.[18] A representative compound of this class, $Ta_6Te_5$, consists of isolated pentagonal antiprismatic Ta chains.[19] Here, the sixth Ta atom is in the center of the column and plays the role of Cd in our cluster. Similar to ${}^1_\infty[Tl_{10}^{10-}]$, the number of electrons per $Ta_6$ unit is also 20 (Te in oxidation state $-2$). However, an isolobal approach is difficult to develop because d orbitals are responsible for the Ta−Ta bonds in $Ta_6Te_5$. Still it is evident that one of the d orbitals on each peripheral Ta is needed to bind tellurium, leaving four d orbitals for the cluster MO's that can be classified in radial and tangential MO's as was done here. A detailed analysis is beyond the scope of this work and can be found in ref 19.

(17) Franzen, H. F.; Smeggil, J. G. *Acta Crystallogr.* **1970**, *B26*, 125.
(18) Harbrecht, B. *J. Less-Common Met.* **1988**, *138*, 225. Degen, T.; Harbrecht, B. *Acta Crystallogr.* **1995**, *C51*, 2218. Conrad, M.; Harbrecht, B. *Z. Anorg. Allg. Chem.* **1997**, *623*, 742. Kim, S. J.; Nanjundaswamy, K. S.; Hughbanks, T. *Inorg. Chem.* **1991**, *30*, 159.
(19) Conrad, M. Ph.D. Dissertation, Universität Dortmund, Dortmund, Germany, 1997.

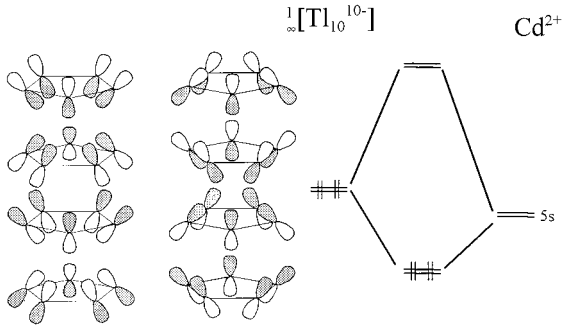


**Figure 5.** Stabilization of the folded p-type $a_1$ band at X from interaction with Cd 5s orbitals.

The overall mixing scheme of the p orbitals (Figure 4) reflects structural characteristics of the new cluster column. The Tl−Tl bond distances within the pentagonal planes become relatively long compared with those both in other clusters[5,15] and in the bonds between five rings in this chain (Figure 1). This is a consequence of band mixing; the $a_z$ and $e_z$ states become partly $\sigma$-bonding between two rings at an expense of radial $a_r$ and $e_r$ states, which become partly antibonding and are therefore unoccupied. Also, the bonding $e_2$ band has contributions from $e_r$* and $e_z$* that are antibonding with respect to Tl−Tl bonds in one ring. The interaction along the chain (*a* axis) is therefore responsible for the expansion of the five-membered rings (compared, for example, with the $\sim D_{5h}$ $Tl_7^{7-}$ recently described[20]).

When the centered Cd atom is included in the calculations, its s and $p_z$ orbitals lower the two bonding $a_1$ bands, and two new nondegenerate bands appear above the Fermi level. At the same time, the $p_x$ and $p_y$ orbitals of Cd lower the bonding $e_1$ crystal orbitals, and a $e_1$ band above the Fermi level is the result. The most effective impact in terms of energy is the lowering of the p type $a_1$ band at the X point. This interaction is depicted in Figure 5. The result is similar to those with other centered atoms,[5] where $Cd^{2+}$ contributes no new orbitals or electrons. The charge transfer between cadmium and thallium is small as indicated by the Mulliken charge for Cd (+0.07), whereas the charges for Tl atoms range between −0.30 and −0.56 with the exception of Tl1 (−0.07) and Tl7 (−0.99). The Cd−Tl bonds are largely covalent rather than ionic in character because of the small differences of their orbital energies.

The acentric Tl7 atom is a key feature of the bonding in $A_5Cd_2Tl_{11}$. As was just noted, one of its effects is to remove charge from the chain. The symmetry of the pentagonal antiprismatic chain is lowered from $D_{5h}$ to $C_s$, and, of course, an additional s band from Tl7 appears below the Fermi level. The e bands split into a′ and a″ bands (symmetric and antisymmetric with respect to the retained mirror plane). This is especially important for the e bands near the Fermi level. Figure 6 shows the splitting of the bonding $2e_2$ crystal orbital at Γ that is mainly of $e_z$* type and how $p_z$ of Tl7 stabilizes a′, strengthening the bonds along *z*. Figure 7 shows the interaction of the $3e_1$ band with $p_y$ of Tl7 at Γ and how the attachment of Tl7 to the chain lengthens the Tl3−Tl3 bonds between the skeletal atoms. The overlap population of the capped edge decreases from 0.19 to 0.14. In fact, in the real structure the capped edge is longer than all other bonds in the five-membered ring. Finally, Figure 8 shows the band diagram near $E_F$ for (left) the $Tl_{10}^{10-}$ chain and (right) the observed $[Cd_2Tl_{11}^{5-}]$. Crossing of two e bands ($3e_1$ and $2e_2$) is avoided in the observed $Cd_2Tl_{11}^{5-}$ chain by mixing bands with the same symmetry,

(20) Kaskel, S.; Corbett, J. D. *Inorg. Chem.* **2000**, *39*, 778.

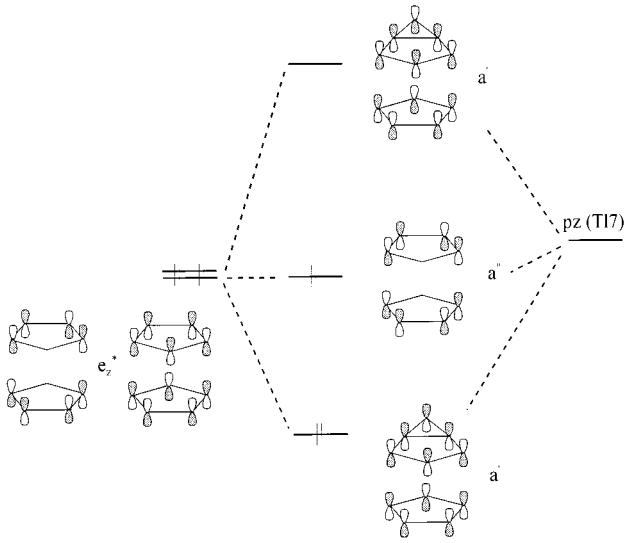


**Figure 6.** Impact of Tl7. The degeneracy of the $e_z$* band is destroyed because of $\pi$-type in-plane interactions and $\sigma$ bonding parallel to the column axis.

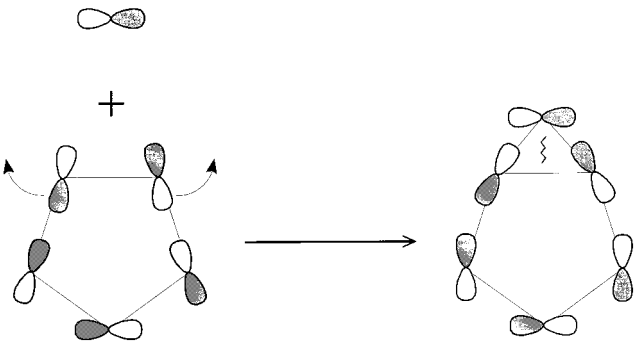

**Figure 7.** $\sigma$ bonds to Tl7 formed in the plane of the five-membered ring result in an opening of the capped Tl3−Tl3 edge via antibonding interactions.

which results in a very small calculated band gap. The cumulative overlap populations are clearly increased through the increased bonding, and the $E_F$ at 42 electrons clearly separates bonding and antibonding states, whereas it falls somewhat above some antibonding states in $Cd_2Tl_{10}^{6-}$.

The effect of Tl7 can be interpreted as a chemical Jahn−Teller type distortion. A degeneracy at the Fermi level is avoided by the additional Tl7 atom that destroys the centricity, stabilizes the bonding states, and enhances the distortion. Although the conversion illustrated in Figure 8 can be stoichiometrically described in terms of the reaction $[Tl_{10}^{10-}] + 2Cd^{2+} + Tl^{+} \rightarrow Tl_{11}Cd_2^{5-}$, there is considerable transfer of charge through bonding back onto the added atoms. This effect is general throughout other centered and condensed cluster anions of the triel elements.[5]

**Properties.** According to our measurements $Cs_5Cd_2Tl_{11}$ has a low electrical resistivity ($\sim$11 $\mu\Omega$ cm) with a positive temperature coefficient, but it is also diamagnetic ($\chi_{296} = 0.84 \times 10^{-4}$ emu mol$^{-1}$). The corresponding properties of the Rb salt are similar, $\sim$24 $\mu\Omega$ cm and $\sim 4.5 \times 10^{-4}$ emu mol$^{-1}$ (Experimental Section). According to our band structure calculations, the anion has a very small electronic band gap, but the limitations of the EHMO method must be kept in mind. The experimental results seem to be in contradiction because we would have expected Pauli paramagnetic behavior for a metallic phase. Even though many aspects can be responsible for the observed measurements (including experimental problems), similar observations pertain to elemental Bi, Pb, and Tl where the conduction electrons are tightly bound and $m_e$ in the free electron model has to be replaced by a much smaller effective mass $m_e$*. The diamagnetic Landau susceptibility thus overweights the Pauli term.[21] Since the valence and conduction bands in $A_5Cd_2Tl_{11}$ are tightly bound and far away from the free electron model, the compound appears to be metallic but diamagnetic. Similar contrasting results have also been found for a considerable number of other thallium and indium cluster network phases[22] and appear to be more generic in kind. Diamagnetic corrections for Langevin terms are uncertain in such a chain, but their omission presumably leaves the diamagnetism overweighted.

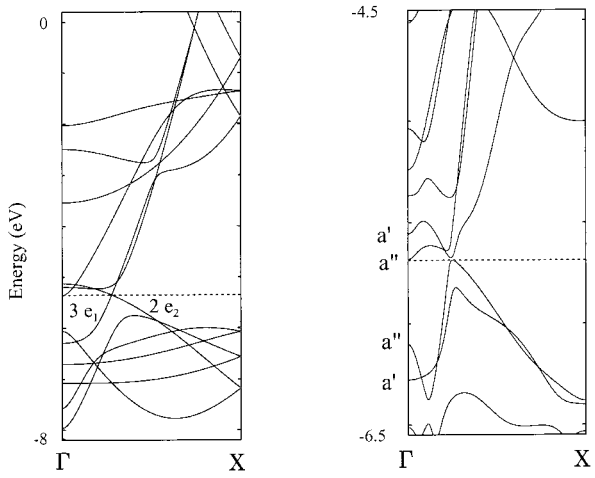


**Figure 8.** Dispersion diagrams for the p bonds near $E_F$ in (left) the $Tl_{10}^{10-}$ chain and (right) the observed $Cd_2Tl_{11}^{5-}$ geometry. The avoided band crossing on the right is the source of the almost zero band gap.

## Conclusions

The discovery of $A_5Cd_2Tl_{11}$, A = Cs, Rb, shows more clearly than any previous example that strong relationships exist between typical *intermetallic* phases, even Ta-rich tellurides, and main-group element cluster anions. Intermetallic compounds can often be viewed as condensed assemblies of cluster molecules. The structural theme of the isolated pentagonal column is interesting on its own, nonetheless, because of the increasing interest in quasicrystalline compounds.[23] If it becomes possible to synthesize columns without the additional acentric atom, the pentagonal columns might be ideal for building a two-dimensional quasi-crystalline packing.

**Acknowledgment.** We thank D.-K. Seo and H. F. Franzen for helpful discussions. The Alexander von Humboldt Foundation provided a Feodor Lynen Fellowship for S. Kaskel. J. Ostenson measured the magnetic data.

**Supporting Information Available:** Tables of additional refinement data and anisotropic displacement parameters for $Cs_5Cd_2Tl_{11}$ and $Rb_5Cd_2Tl_{11}$, plots of magnetic susceptibility and electrical resistivity data as a function of temperature for both compounds, and additional figures cited in the development of the extended Hückel band description. This material is available free of charge via the Internet at http://pubs.acs.org.

IC000061Y

(21) Elliott, S. *The Physics and Chemistry of Solids*; John Wiley & Sons: Chichester, U.K., 1998.
(22) Reference 5a, p 172.
(23) Janot, C., Ed. *Quasicrystals, A Primer*, 2nd ed.; Clarendon Press: Oxford, 1994.